Comparison of Scalar and Vector Modeling of Image Formation in Photoresist

Chris A. Mack, FINLE Technologies, Inc.
Ching-Bo Juang, The University of Texas at Austin*

* present address: Silicon Valley Group, Austin, TX

Abstract

A comparison is made between several scalar models for the formation of an image in a photoresist film with differing approximations and a vector model. It was found that up to numerical apertures of 0.7, a full scalar model showed no appreciable deviation from the vector model. However, when several common assumptions were made to simplify the scalar model, significant errors resulted at the higher numerical apertures.

Keywords: microlithography, lithography modeling, image modeling, PROLITH/2

I. Introduction

Since the first description of lithographic image formation in mathematical terms, lithographers have grappled with the tradeoffs between the ease and speed of simple calculations and the accuracy of more complex calculations. Modeling of the formation of an image and the propagation of that image into photoresist can range from scalar diffraction theory with a variety of approximations to full vector diffraction theory. Recent work has shown that complex vector diffraction theory can be applied to the problem of lithographic image formation, but at a heavy cost in terms of the complexity of the model and the speed of execution. There has been little work, however, in determining the need for such complexity. In particular, if vector theory provides more accurate results at high numerical apertures, at what numerical aperture would the use of vector models become necessary? What other conditions might necessitate the use of a vector image model?

In this paper, several scalar models, with a variety of approximations, will be compared with a vector model. In a two-dimensional case, the goal is to determine the intensity of light everywhere within the photoresist, $I(x,z)$. A full scalar solution is quite accurate in most cases, but usually the "scalar" models used in most studies make one or more approximations to simplify and speed the calculations. First, each of several approximations to a full scalar model of lithographic exposure will be explained. Then, each model will be compared under several conditions of feature size and numerical aperture to determine which models are accurate under what conditions.

0-8194-1788-2/95/$6.00

Downloaded From: http://proceedings.spiedigitallibrary.org/ on 06/02/2014 Terms of Use: http://spiedl.org/terms

Description of the Models

It is not sufficient to describe a lithography imaging model as being simply "scalar" or "vector." Within these broad categories there are a number of different approximations that can be made to simplify the calculations. Several of these approximations are described below.

Zero Order Scalar Model

The lithography simulator SAMPLE [1] and the 1985 version of PROLITH [2] used the simple imaging approximation first proposed by Dill [3] to calculate the propagation of an aerial image in photoresist. First, an aerial image $I_i(x)$ is calculated as if projected into air (x being along the surface of the wafer and perpendicular to the propagation direction of the image). Second, a standing wave intensity $I_s(z)$ is calculated assuming a plane wave of light is normally incident on the photoresist coated substrate (where z is defined as zero at the top of the resist and is positive going into the resist). Then, it is assumed that the actual intensity within the resist film $I(x,z)$ can be approximated by

$$I(x,z) \approx I_i(x) I_s(z) \quad (1)$$

For very low numerical apertures and reasonably thin photoresists, these approximations are valid. They begin to fail when the aerial image changes as it propagates through the resist (i.e., it defocuses) or when the light entering the resist is appreciably non-normal.

First Order Correction to the Scalar Model

The first attempt to correct one of the deficiencies of the zero order model was made by the author [4], and later by Bernard [5]. The aerial image, while propagating through the resist, is continuously changing focus. Thus, even in air, the aerial image is a function of both x and z. An aerial image simulator calculates images as a function of x and the distance from the plane of best focus, δ. Letting δ_o be the defocus distance of the image at the top of the photoresist, the defocus within the photoresist at any position z is given by

$$\delta(z) = \delta_o + \frac{z}{n} \quad (2)$$

where n is the real part of the index of refraction of the photoresist. The intensity within the resist is then given by

$$I(x,z) = I_i(x,\delta(z)) I_s(z) \quad (3)$$

Downloaded From: http://proceedings.spiedigitallibrary.org/ on 06/02/2014 Terms of Use: http://spiedl.org/terms

Here the assumption of normally incident plane waves is still used when calculating the standing wave intensity. This approximate form of the scalar model is known as the "Standard Model" in the lithography simulator PROLITH/2.

Second Order Correction to the Scalar Model

The light propagating through the resist can be thought of as various plane waves traveling through the resist in different directions. Consider first the propagation of the light in the absence of diffraction by a mask pattern (that is, exposure of the resist by a large open area). The spatial dimensions of the light source determine the characteristics of the light entering the photoresist. For the simple case of a coherent point source of illumination centered on the optical axis, the light traveling into the photoresist would be the normally incident plane wave used in the calculations presented above. The standing wave intensity within the resist can be determined analytically [6] as the square of the magnitude of the electric field given by

$$E(z)=\frac{\tau_{12}E_I\left(e^{-i2\pi \mathbf{n}_2 z/\lambda}+\rho_{23}\tau_D^2\, e^{i2\pi \mathbf{n}_2 z/\lambda}\right)}{1+\rho_{12}\rho_{23}\tau_D^2} \tag{4}$$

where the subscripts 1, 2, and 3 refer to air, the photoresist and the substrate, respectively, D is the resist thickness, E_I is the incident electrical field, λ is the wavelength, and where

complex index of refraction of film j: $\mathbf{n}_j = n_j - i\kappa_j$

transmission coefficient from i to j: $\tau_{ij}=\dfrac{2\mathbf{n}_i}{\mathbf{n}_i+\mathbf{n}_j}$

reflection coefficient from i to j: $\rho_{ij}=\dfrac{\mathbf{n}_i-\mathbf{n}_j}{\mathbf{n}_i+\mathbf{n}_j}$

internal transmittance of the resist: $\tau_D = e^{-i2\pi \mathbf{n}_2 D/\lambda}$

The above expression can be easily modified for the case of non-normally incident plane waves. Suppose a plane wave is incident on the resist film at some angle θ_I. The angle of the plane wave inside the resist will be θ_2 as determined from Snell's law. An analysis of the propagation of this plane wave within the resist will give an expression similar to equation (4) but with the position z replaced with $z\cos\theta_2$.

$$E(z,\theta_2)=\frac{\tau_{12}(\theta_2)E_I\left(e^{-i2\pi \mathbf{n}_2 z\cos\theta_2/\lambda}+\rho_{23}(\theta_2)\tau_D^2(\theta_2)\, e^{i2\pi \mathbf{n}_2 z\cos\theta_2/\lambda}\right)}{1+\rho_{12}(\theta_2)\rho_{23}(\theta_2)\tau_D^2(\theta_2)} \tag{5}$$

The transmission and reflection coefficients are now functions of the angle of incidence and are given by the Fresnel formulas. They are also a function of the polarization of the incident light. For the typical unpolarized case, the light entering the resist will become polarized (but only slightly).

Downloaded From: http://proceedings.spiedigitallibrary.org/ on 06/02/2014 Terms of Use: http://spiedl.org/terms

Thus, a separate standing wave can be calculated for each polarization and the resulting intensities summed to give the total intensity. A similar approach was taken by Bernard and Urbach [7]. Notice that by using a more accurate scalar model, vector effects such as polarization within the resist film still come into play.

By calculating the standing wave intensity at one incident angle θ_1 to give $I_s(z,\theta_1)$, the full standing wave intensity can be determined by integrating over all angles. Each incident angle comes from a given point in the illumination source, so that integration over angles is the same as integration over the source. Thus, the effect of partial coherence on the standing waves is accounted for. Note that the effect of the non-normal incidence is included only with respect to the zero order light (the light which is not diffracted by the mask). This form of the scalar imaging problem is known as the "High NA Scalar" model in PROLITH/2.

Full Scalar Model

The above method for calculating the image intensity within the resist still makes the assumption of separability, that an aerial image and a standing wave intensity can be calculated independently and then multiplied together to give the total intensity. This assumption is not required. Instead, one could calculate the full $I(x,z)$ at once making only the standard scalar approximation. The formation of the image can be described as the summation of plane waves. For coherent illumination, each diffraction order gives one plane wave propagating into the resist. Interference between the zero order and the higher orders produces the desired image. Each point in the illumination source will produce another image which will add incoherently (i.e., intensities will add) to give the total image. Equation (5) describes the propagation of a plane wave in a stratified media at any arbitrary angle. By applying this equation to each diffraction order, an exact scalar representation of the full intensity within the resist is obtained.

Other Issues in Scalar Modeling

Besides the basic modeling approaches described above, there are two issues which apply to any model. First, the effects of defocus are taken into account by describing defocus as a phase error at the pupil plane. Essentially, if the curvature of the wavefront exiting the objective lens pupil is such that it focuses in the wrong place (i.e., not where you want it), one can consider the wavefront curvature to be wrong. Simple geometry then relates the optical path difference (OPD) of the actual wavefront from the desired wavefront as a function of the angle of the light exiting the lens, θ.

$$OPD(\theta) = \delta(1 - \cos\theta) \qquad (6)$$

Computation of the imaging usually involves a change in variables where the main variable used is $\sin\theta$. Thus, the cosine adds some algebraic complexity to the calculations. For this reason, it is common in optics texts to simplify the OPD function for small angles (i.e., low numerical apertures).

Downloaded From: http://proceedings.spiedigitallibrary.org/ on 06/02/2014 Terms of Use: http://spiedl.org/terms

$$OPD(\theta) = \delta(1-\cos\theta) \approx \frac{\delta}{2}\sin^2\theta \qquad (7)$$

Again, the approximation is not necessary, and is only made to simplify the resulting equations. In this work, the approximate defocus expression is used for the zero order model and the first order correction. The second order correction and the full scalar model use the exact defocus expression.

Reduction in the imaging system adds an interesting complication. Light entering the objective lens will leave the lens with no loss in energy (the lossless lens assumption). However, if there is reduction in the lens, the *intensity* of the light entering will be different from that leaving since the intensity is the energy spread over a changing area. The result is a radiometric correction well known in optics [8] and first applied to lithography by Cole and Barouch [9]. In this work, the radiometric correction is applied in the second order correction and the full scalar models.

Vector Model

Light is an electromagnetic wave which can be described by time-varying electric and magnetic field vectors. In lithography, the materials used are generally non-magnetic so that only the electric field is of interest. The electric field vector is described by its three vector components. Maxwell's equations, sometimes put into the form of the wave equation, govern the propagation of the electric field vector. The *scalar approximation* assumes that each of the three components of the electric field vector can be treated separately as scalar quantities and each scalar electric field component must individually satisfy the wave equation.

The scalar approximation is commonly used throughout optics and is known to be accurate under many conditions. There is one simple situation, however, in which the scalar approximation is not adequate. Consider the interference of two plane waves traveling past each other. If each plane wave is treated as a vector, they will interfere only if there is some overlap in their electric field vectors. If the vectors are parallel, there will be complete interference. If, however, their electric fields are at right angles to each other there will be no interference. The scalar approximation essentially assumes that the electric field vectors are always parallel and will always give complete interference. This situation comes into play in lithography when considering the propagation of plane waves traveling through the resist at large angles. Reflection of a plane wave from the substrate will give two plane waves traveling past each other at some angle. For large angles, the scalar approximation may fail to account for these vector effects.

For this work, the vector model technique of Flagello [10] was used. The software used to perform the vector solution was developed by Tim Brunner of IBM and is used here to compare with the various forms of the scalar model. Note that the Flagello/Brunner model accounts for vector propagation of the light in the photoresist, but uses scalar theory to describe diffraction by the mask, and the behavior of the imaging lens. Also, this software does not take into account any changes in the optical properties of the photoresist during exposure (i.e., bleaching). Both polarized or unpolarized illumination can be modeled.

Downloaded From: http://proceedings.spiedigitallibrary.org/ on 06/02/2014 Terms of Use: http://spiedl.org/terms

Comparison of Models

There is a wide number of possible conditions that could be explored to look for differences between the various imaging models. Here, only a small number of representative conditions will be studied. In particular, i-line (365 nm) imaging of 0.35 and 0.50 µm equal lines and spaces with numerical apertures of 0.5, 0.6 and 0.7 will be simulated through focus. Unpolarized illumination is assumed. The complete set of modeling parameters is shown in Table I. All of the models described above will be compared with the exception of the zero order model, since the inaccuracies of this model are already well known.

Table I. PROLITH/2 input parameters

Imaging Tool:	CEL or Top ARC:
Wavelength = 365.0 nm	Not Used
Bandwidth = 0.0 nm	Intermediate Layers: Polysilicon on oxide
Numerical Aperture = 0.5, 0.6 and 0.7	Substrate: Silicon
Reduction Ratio = 5.0	
Image Flare = 0.00	Resist System: Positive
Aberrations: None	Thickness = 0.800 µm
Partial Coherence = .50	Absorption Parameter A = 0.00 1/µm
Linewidth = 0.35 and 0.50 µm	Absorption Parameter B = 0.50 1/µm
Pitch = 2*width	Rate Constant C = 0.0160 cm^2/mJ
Mask Bias = 0.0 µm	Refractive Index = 1.755
Focal Position = -0.30 µm	Development Model: Original Mack
	Max Develop Rate = 100.0 nm/s
	Min Develop Rate = 0.10 nm/s
Exposure Energy = 160 mJ/cm^2	Threshold M = -100.
PEB Diffusion length = 60.0 nm	Selectivity Parameter n = 5.00
Development Time = 60.0 sec	Relative Surface Rate = 0.10
	Inhibition Depth = 0.10 µm

Figure 1 begins by comparing resist profiles at two extremes of focus (the in-focus profiles show the least variation among the models and so are not shown here). Several points can be made. First, all of the models shown exhibit the same asymmetry with focus. The simplest model, the first order correction (standard model) which accounts for defocusing within the resist, is sufficient to explain this basic phenomenon. The asymmetry certainly worsens for larger numerical apertures. Comparing the different models, one sees in all cases the greatest difference between the standard and the high NA scalar models. There is a smaller but noticeable difference between the high NA and full scalar models. There appears to be very little difference between the full scalar and the vector models. As one would expect, the differences between the models becomes more

Downloaded From: http://proceedings.spiedigitallibrary.org/ on 06/02/2014 Terms of Use: http://spiedl.org/terms

pronounced at higher numerical apertures. There seems to be neither more nor less differences between the models for the 0.5 μm versus the 0.35 μm feature sizes.

Figure 2 expands on this data by showing linewidth versus focus results for the different models at different numerical apertures. Even at a numerical aperture of 0.5 there is a noticeable difference between the standard and the high NA scalar models. Interestingly, the difference resembles a difference in dose, indicating that the inclusion of the full angular range of the incident light reduces the swing curve effect and changes the amount of energy coupled into the resist. At numerical apertures of 0.5 and 0.6, the differences between the high NA scalar and full scalar models are not great, but the high NA scalar model does underestimate the focus latitude on the negative side of focus (focal plane position below the top surface of the resist). At a numerical aperture of 0.7, the high NA scalar model results begin to deviate from the full scalar model at positive focus. For all numerical apertures, the full scalar model and the vector model show very little difference.

Conclusions

The differences between "scalar" and "vector" models are impossible to judge without a thorough understanding of the assumptions made in each model. In fact, at numerical apertures up to, and probably beyond, 0.7 variations among the scalar models with different assumptions far exceed any error caused by making the scalar approximation. For the cases studied in this paper, there were only insignificant differences between the full scalar and vector models at numerical apertures up to 0.7. There were, however, significant differences between the various scalar models. The standard model gives qualitative agreement with the high NA asymmetries found in the other models, but begins to show quantitative differences at numerical apertures above 0.5. The high NA scalar model is more accurate and shows good results up to numerical apertures of about 0.6. In all cases, the differences between models look like differences in dose and result from improved accounting of the influence of NA on thin film interference effects.

Further work in this area should certainly be undertaken. More numerical apertures, both higher and lower, should be studied. Full focus-exposure process windows should be calculated and compared. Further, the results presented here indicate that the proper inclusion of high angles in the scalar model is needed for accurate results. Thus, one would suspect that off-axis illumination imaging would be affected substantially. Further work should include a wide range of off-axis illumination and phase-shifting mask cases and should study swing curve effects explicitly.

Acknowledgments

The author wishes to thank Tim Brunner of IBM for the use of his vector imaging model.

Downloaded From: http://proceedings.spiedigitallibrary.org/ on 06/02/2014 Terms of Use: http://spiedl.org/terms

References

1. W. G. Oldham, S. N. Nandgaonkar, A. R. Neureuther and M. O'Toole, "A General Simulator for VLSI Lithography and Etching Processes: Part I - Application to Projection Lithography," *IEEE Trans. Electron Dev.*, ED-26, No. 4 (April 1979) pp. 717-722.

2. C. A. Mack, "PROLITH: A Comprehensive Optical Lithography Model," *Optical Microlith. IV, Proc.*, SPIE Vol. 538 (1985) pp. 207-220.

3. F. H. Dill, A. R. Neureuther, J. A. Tuttle, and E. J. Walker "Modeling Projection Printing of Positive Photoresists," *IEEE Trans. Electron Dev.*, ED-22, No. 7, (1975) pp. 456-464.

4. C. A. Mack, "Understanding Focus Effects in Submicron Optical Lithography," *Optical/Laser Microlithography, Proc.*, SPIE Vol. 922 (March, 1988) pp. 135-148, and *Optical Engineering*, Vol. 27, No. 12 (Dec. 1988) pp. 1093-1100.

5. D. A. Bernard, "Simulation of Focus Effects in Photolithography," *IEEE Trans. Semiconductor Manufacturing*, Vol. 1, No. 3 (August, 1988) pp. 85-97.

6. C. A. Mack, "Analytical Expression for the Standing Wave Intensity in Photoresist", *Applied Optics*, Vol. 25, No. 12 (15 June 1986) pp. 1958-1961.

7. D. A. Bernard and H. P. Urbach, "Thin-film Interference Effects in Photolithography for Finite Numerical Apertures," *Jour. Optical Society of America A*, Vol. 8, No. 1 (Jan., 1991) pp. 123-133.

8. M. Born and E. Wolf, Principles of Optics, 6th edition, Pergamon Press, (Oxford, 1980) pp. 113-117.

9. D. C. Cole, E. Barouch, U. Hollerbach, and S. A. Orszag, "Extending Scalar Aerial Image Calculations to Higher Numerical Apertures," Jour. Vacuum Science and Tech., Vol. B10, No. 6 (Nov/Dec, 1992) pp. 3037-3041.

10. D. G. Flagello, A. E. Rosenbluth, C. Progler, J. Armitage, "Understanding High Numerical Aperture Optical Lithography," *Microelectronic Engineering*, Vol 17 (1992) pp. 105-108.

Downloaded From: http://proceedings.spiedigitallibrary.org/ on 06/02/2014 Terms of Use: http://spiedl.org/terms

NA = 0.5 | **Focus = -1.0 µm** | **Focus = 0.6 µm**

Standard Model

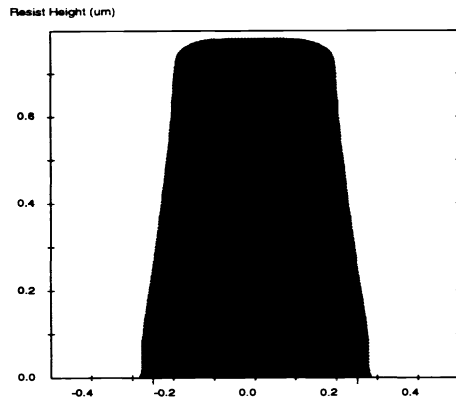

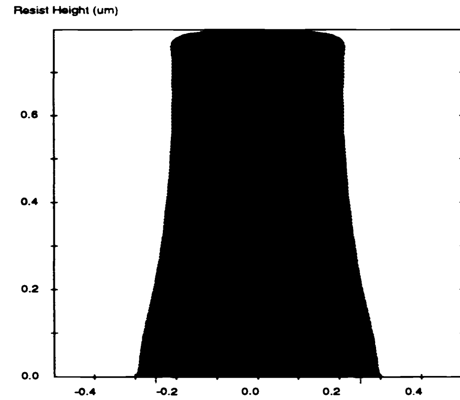

High NA Scalar

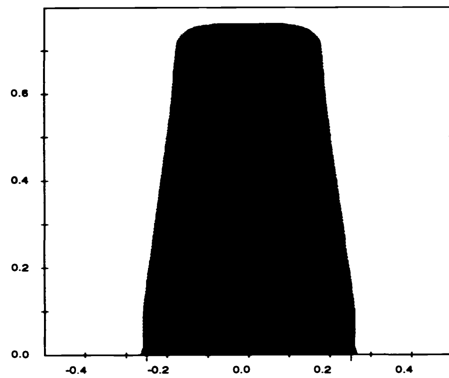

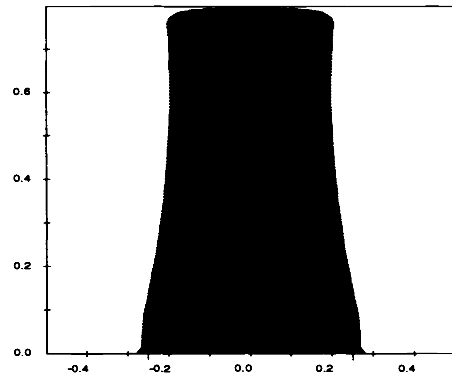

Full Scalar

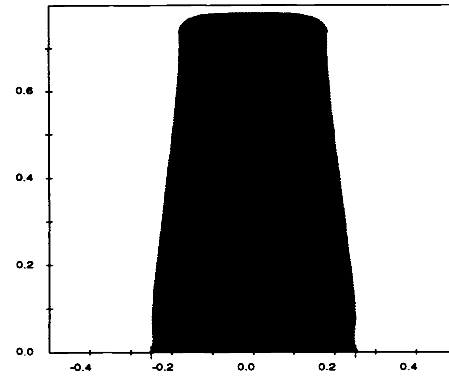

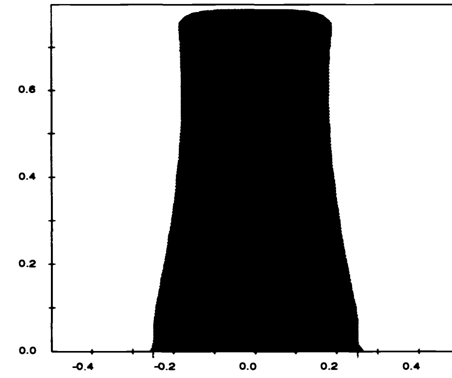

Vector Model

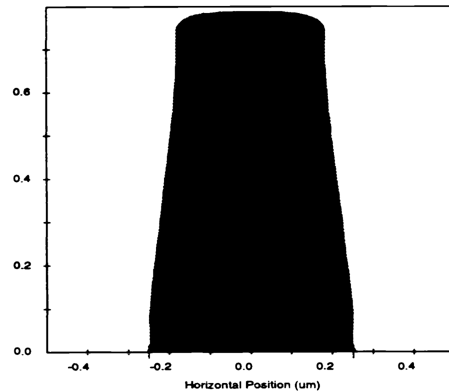

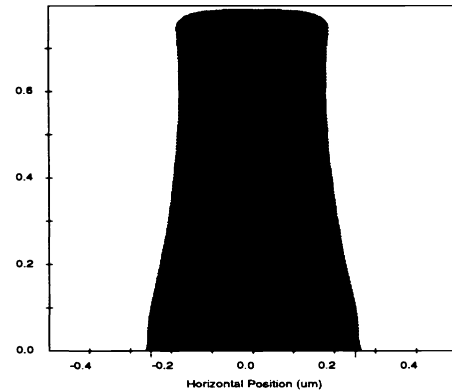

Figure 1a. Comparison of models for 0.5 µm lines and spaces with NA = 0.5, i-line, σ = 0.5.

Downloaded From: http://proceedings.spiedigitallibrary.org/ on 06/02/2014 Terms of Use: http://spiedl.org/terms

NA = 0.6 **Focus = -1.0 μm** **Focus = 0.6 μm**

Standard Model

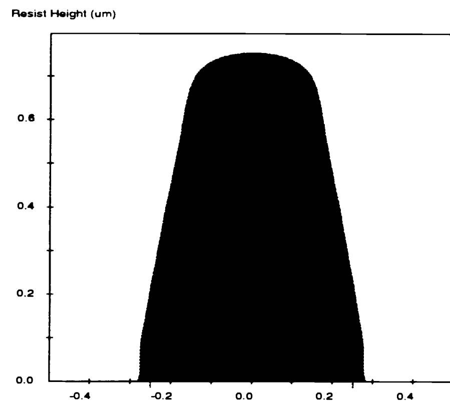

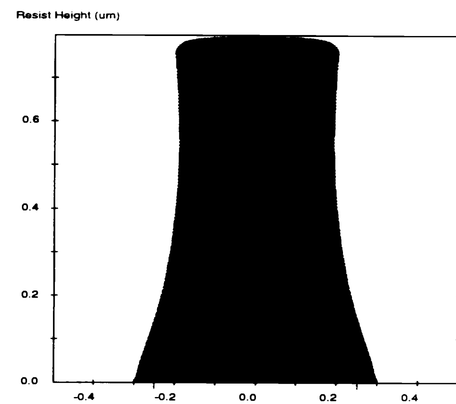

High NA Scalar

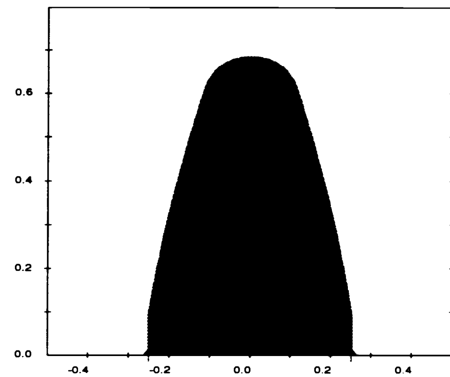

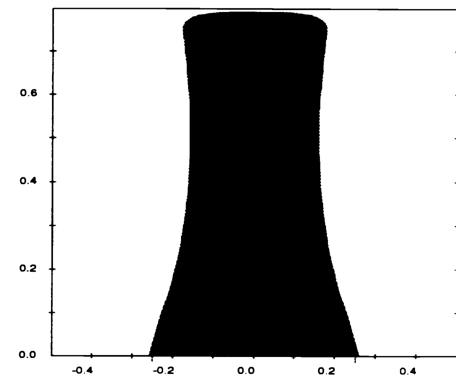

Full Scalar

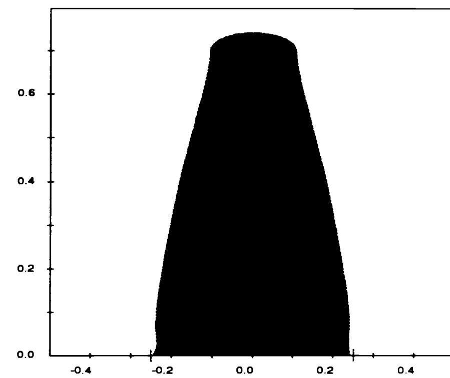

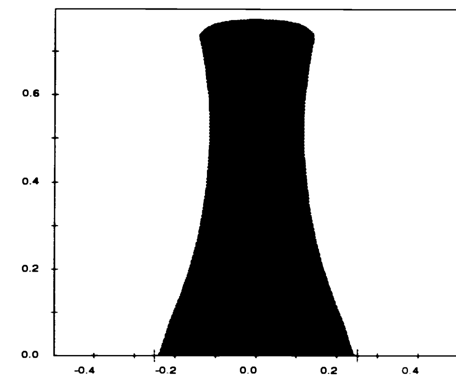

Vector Model

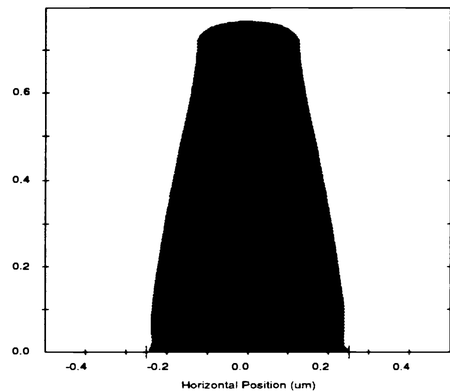

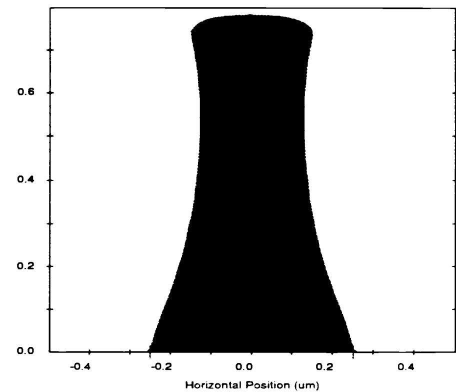

Figure 1b. Comparison of models for 0.5 μm lines and spaces with NA = 0.6, i-line, σ = 0.5.

Downloaded From: http://proceedings.spiedigitallibrary.org/ on 06/02/2014 Terms of Use: http://spiedl.org/terms

NA = 0.7 **Focus = -1.0 μm** **Focus = 0.6 μm**

Standard Model

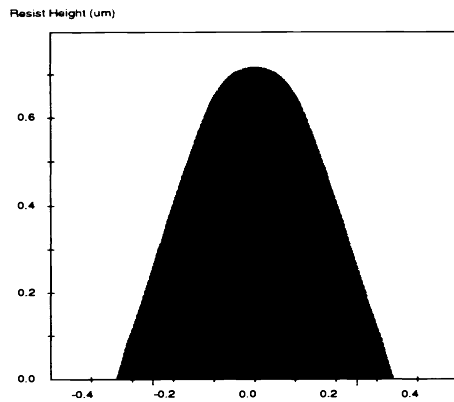

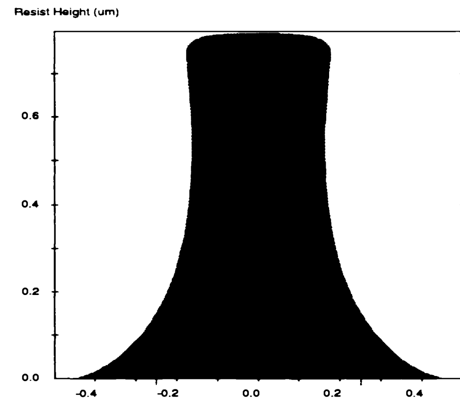

High NA Scalar

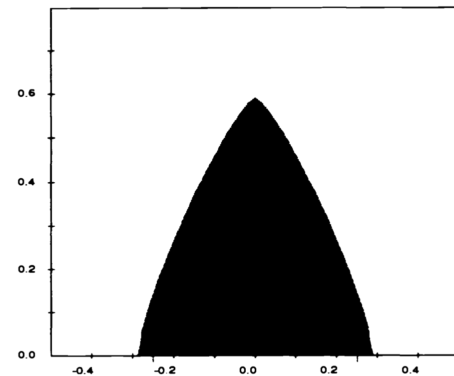

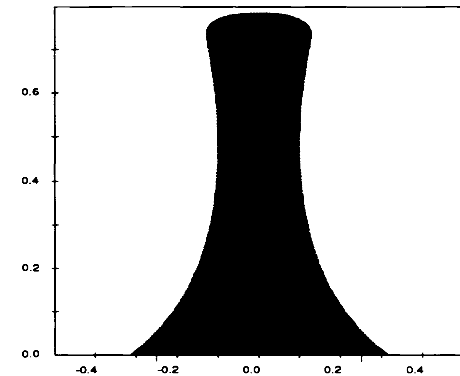

Full Scalar

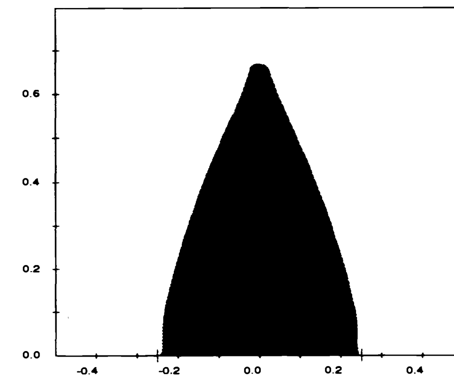

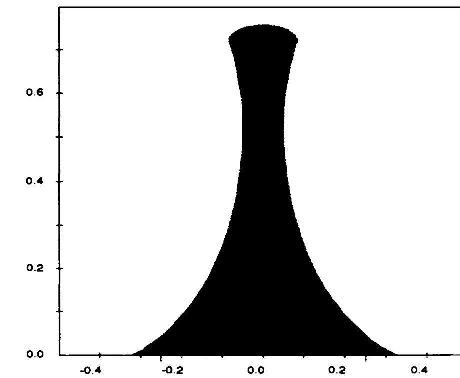

Vector Model

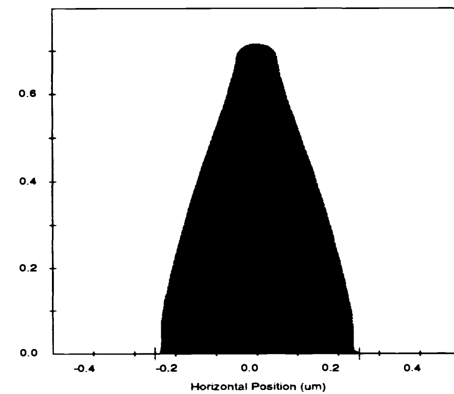

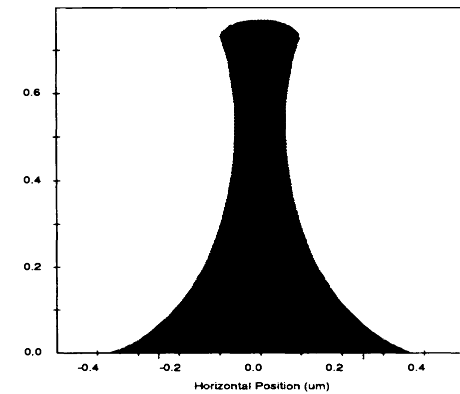

Figure 1c. Comparison of models for 0.5 μm lines and spaces with NA = 0.7, i-line, $\sigma = 0.5$.

Downloaded From: http://proceedings.spiedigitallibrary.org/ on 06/02/2014 Terms of Use: http://spiedl.org/terms

NA = 0.6 | **Focus = -0.6 μm** | **Focus = 0.2 μm**

Standard Model

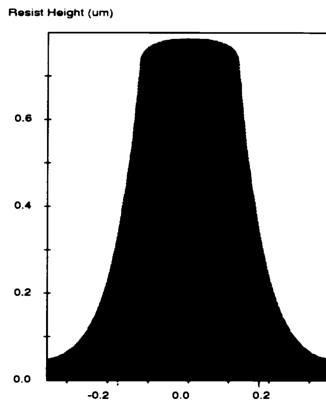

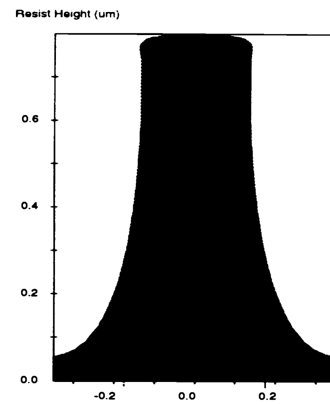

High NA Scalar

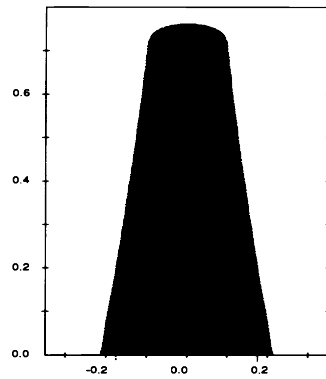

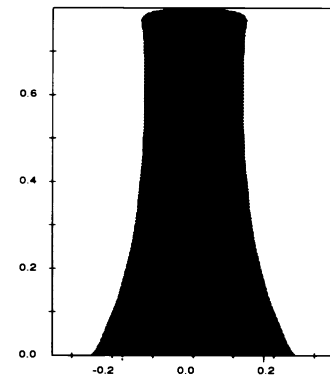

Full Scalar

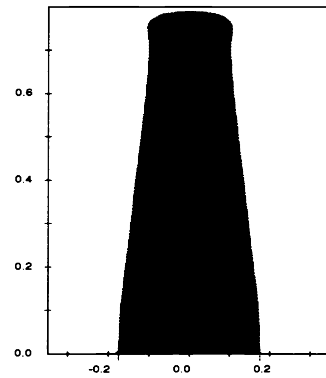

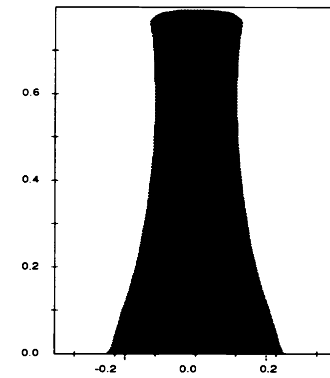

Vector Model

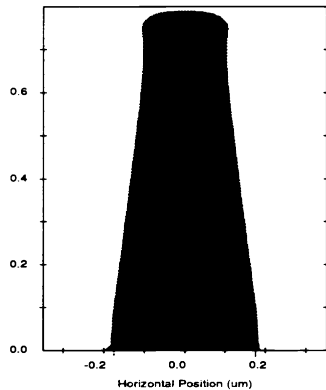

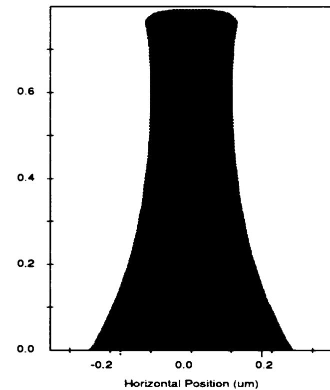

Figure 1d. Comparison of models for 0.35 μm lines and spaces with NA = 0.6, i-line, $\sigma = 0.5$.

Downloaded From: http://proceedings.spiedigitallibrary.org/ on 06/02/2014 Terms of Use: http://spiedl.org/terms

NA = 0.7 | **Focus = -0.6 μm** | **Focus = 0.2 μm**

Standard Model

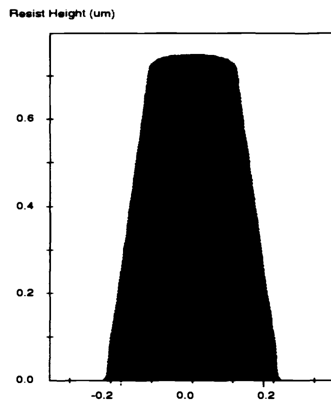

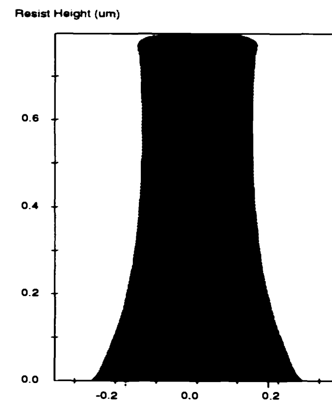

High NA Scalar

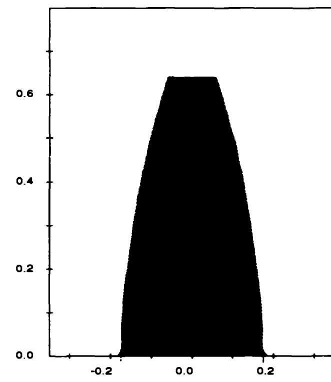

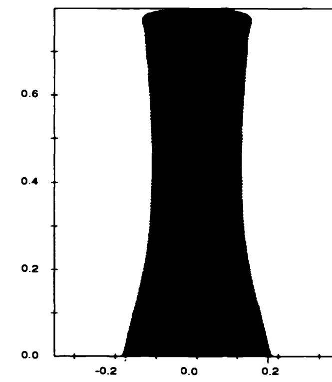

Full Scalar

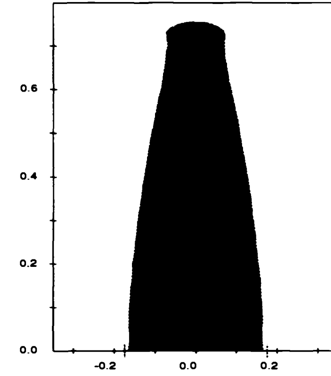

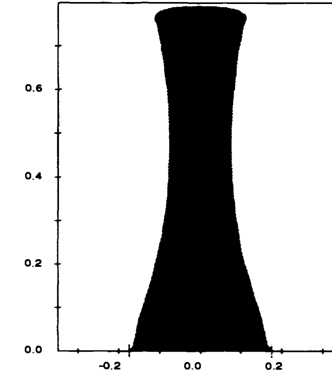

Vector Model

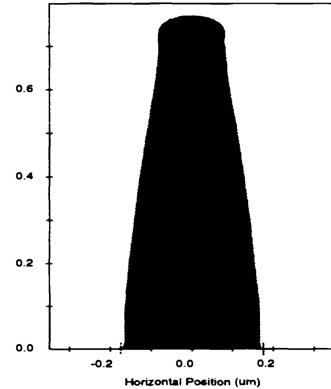

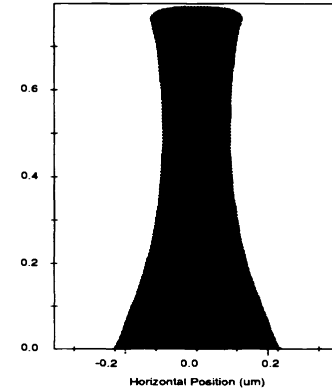

Figure 1e. Comparison of models for 0.35 μm lines and spaces with NA = 0.7, i-line, σ = 0.5.

Downloaded From: http://proceedings.spiedigitallibrary.org/ on 06/02/2014 Terms of Use: http://spiedl.org/terms

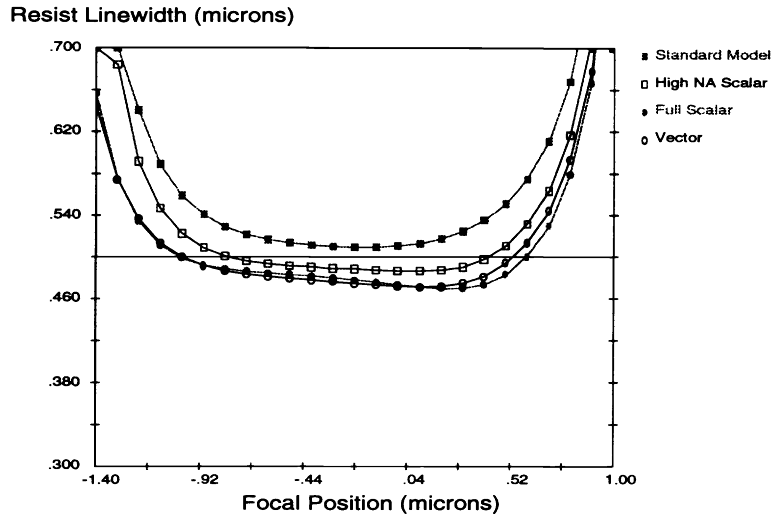

(a)

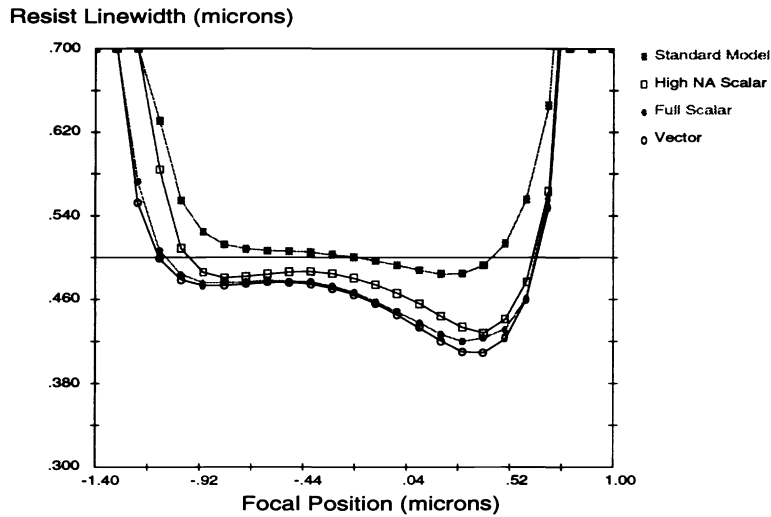

(b)

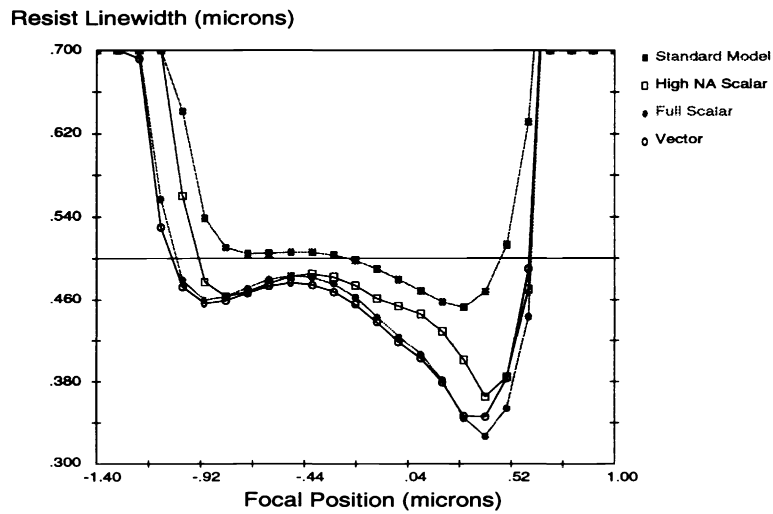

(c)

Figure 2. Comparison of image models for an i-line process with NA of (a) 0.5, (b) 0.6, and (c) 0.7.

Downloaded From: http://proceedings.spiedigitallibrary.org/ on 06/02/2014 Terms of Use: http://spiedl.org/terms